International Journal of Solids and Structures 47 (2010) 2653–2659

Contents lists available at ScienceDirect

International Journal of Solids and Structures

journal homepage: www.elsevier.com/locate/ijsolstr

Thermo-mechanical large deformation responses of Hydrogenated Nitrile Butadiene Rubber (HNBR): Experimental results

Akhtar S. Khan [a], Muneer Baig [b,*], Syed Hamid [c], Hao Zhang [c]

[a] Department of Mechanical Engineering, University of Maryland, Baltimore County, Baltimore, MD 21250, USA
[b] Center of Excellence for Research in Engineering Materials, King Saud University, Riyadh, Saudi Arabia
[c] Research Department, Halliburton Energy Services, Carrollton, TX 75006, USA

ARTICLE INFO

Article history:
Received 22 August 2009
Received in revised form 6 May 2010
Available online 20 May 2010

Keywords:
HNBR
Constitutive behavior
Quasi-static and dynamic response
SHPB

ABSTRACT

A comprehensive study on the large uniaxial deformation responses of two elastomers, Hydrogenated Nitrile Butadiene Rubbers (HNBR A and HNBR B), over wide ranges of strain rates ($10^{-4} \leqslant \dot{\varepsilon} \leqslant 5 \times 10^{3}\ s^{-1}$) and temperatures ($348 \leqslant T \leqslant 450$ K) are presented. The material is found to be non-linearly dependent on strain-rate and temperature. The large deformation responses of HNBR are determined to be almost purely viscoelastic. It is observed that, the instantaneous stress drop during the stress relaxation is dependent on the strain-rate. The relaxation and creep responses during the equilibrium state (a state where there is no drop in stress during relaxation and no increase in strain during creep) are dependent on strain/stress level at which the phenomenon is started.

1. Introduction

Polymers are an important class of engineering materials that consist of many self-repeating smaller units called monomers. The different properties of the polymers are based on arrangement and synthesis of these monomers. Polymers are increasingly used as engineering materials due to their high manufacturability, low weight, low cost and good mechanical properties. In general, they are classified into three major groups-thermoplastics (repeatedly soften when heated and then solidify when cooled), thermosets (sets irreversibly when heated) and elastomers (rubbery polymers that can stretch to several times their initial length and return to its original dimensions when the applied load is released). The material Hydrogenated Nitrile Butadiene Rubber (HNBR) used in the present study is an elastomer. Elastomers in general are used as shock absorbers because of their low modulus and high damping characteristics (Fatt and Ouyang, 2008). HNBRs are widely used in the automotive industry for a multitude of seals, belts and hoses because of its strength and retention of its properties after long term exposure to heat, oil and fuel. They are also used as sealing materials in oil exploration and its processing. Due to their high damping characteristics, elastomers are increasingly used in applications that are subjected to shock, impact and vibrations. Thus, understanding the mechanical behavior of elastomers over a wide range of strain-rates and temperatures could significantly improve the design capabilities of such applications.

Numerous studies (Jerrams et al., 1998; Haupt et al., 2000; Chen et al., 1999; Khan and Zhang, 2001; Khan and Pamies, 2002; Beda, 2007; Khan and Farrokh, 2006; Fatt and Ouyang, 2008; Spathis and Kontou, 2008; Zaïri et al., 2008; Anand et al., 2009; Ames et al., 2009; Regrain et al., 2009) have been performed to characterize the responses of polymeric materials. In order to characterize the material responses at high rates of loading, Chen et al. (1999) made modifications to a conventional split Hopkinson pressure bar (SHPB) to perform high strain-rate compression experiments on low-impedance materials. Quasi-static and dynamic experiments were performed on RTV630 silicon rubber, an elastomer with low compressive strength. The maximum strain-rate and strain achieved in dynamic experiments was 7960 s^{-1} and 79% true strain, respectively. A significant increase in stress at a given level of strain was observed when the strain-rate was changed from quasi-static (2.46 s^{-1}) to dynamic (7960 s^{-1}). Khan and Pamies (2002) performed a comprehensive study on large deformation of an elastomer (Adiprene-L100) over a wide range of strain-rates and temperatures. At room temperature, they observed that Adiprene-L100 exhibited stress relaxation, which was dependent on the strain-rate and level of strain at which the relaxation was started. Also, at room temperature Adiprene-L100 exhibited a change in behavior from "rubbery" to "glassy" when the strain-rate was increased from 1 s^{-1} to 5000 s^{-1}. Bergström and Boyce (1998) investigated the material response of carbon black filled chloroprene and nitrile rubbers at different strain-rates. They observed that the material responses of elastomers are strain-rate dependent; this is more pronounced during the loading than unloading period. They also performed stress relaxation experiments with

* Corresponding author. Tel.: +966 053 413 8089.
E-mail address: bmuneer@ksu.edu.sa (M. Baig).

0020-7683/$ - see front matter © 2010 Elsevier Ltd. All rights reserved.
doi:10.1016/j.ijsolstr.2010.05.012

relaxation periods during unloading. During the relaxation period, the stress was observed to decrease while loading and increase while unloading. Fatt and Ouyang (2008) reported experimental results on styrene butadiene rubber subjected to constant strain-rates ranging from 76 s^{-1} to 450 s^{-1}. These experiments were performed using a Charpy tensile impact apparatus. They observed that the elastomer tends to exhibit "stiffer or glassy" behavior with an increase in strain-rate (a similar observation was made by Khan and Pamies, 2002). The stiffer response of elastomers with increasing strain-rate is believed to be due to an insufficient relaxation time during the loading period (Fatt and Ouyang, 2008).

During the last decade, numerous research papers (Chen et al., 1999; Khan and Zhang, 2001; Khan and Pamies, 2002; Beda, 2007; Bardenhagen et al., 1997; Qi and Boyce, 2005; Khan and Farrokh, 2006; Fatt and Ouyang, 2008; Spathis, 1995; Bird et al., 1977) characterized the response of elastomers. However, the majority of the work is limited to small deformation/or narrow spectrum of strain-rates and temperatures. The present study deals with characterizing the large deformation response of two elastomers over a wide range of strain-rates and temperatures. The present work can be considered to be different from earlier published paper (Khan et al., 2006) where the results reported were only about 60% true strain. The present work can be considered to be different from earlier published paper (Khan et al., 2006) where the results reported were only about 60% true strain. The results of this paper can be considered to be different (or new) from the earlier version because the authors observed highly non-linear responses in case of HNBR polymer after 60% true strain, which were not reported in the earlier study on a different polymer (Adiprene).

2. Experimental procedure

2.1. Material

All the specimens used in this study were made from HNBR cast in a plate. The cylindrical specimens of 25.4 mm (1.0 in.) in diameter and 38 mm (1.5 in.) in length were machined for this purpose. The materials used in the present study, HNBR A and HNBR B are considered as hard and soft, respectively based on their strength.

2.2. Compression experiments at room temperature

Quasi-static monotonic compression experiments were performed at strain-rates ranging from 10^{-4} to 10^{0} s^{-1}. These experiments were performed in the displacement-controlled mode to maintain a constant engineering strain-rate throughout the deformation process. Because of the difficulty in bonding strain gages on the HNBR elastomer, the displacement from the machine was corrected for machine compliance. The corrected displacement was used to calculate the strain. The interface between the test specimen and MTS fixture platens was lubricated with a combination of a Teflon sheet (0.076 mm thickness) and Dow Corning high vacuum grease. This combination of Teflon and grease was sufficient to avoid any possible barreling of the specimen during deformation, thus ensuring a homogeneous deformation and uniform stress state throughout the experiment.

2.3. Quasi static experiments at different temperatures

To investigate the temperature dependency of the materials, the samples were subjected to compressive loading at the strain-rate of 10^{-2} s^{-1} and at temperatures ranging from 348 K to 450 K. The corrected displacement data was used to calculate the strain. High temperature vacuum grease manufactured by Dow Corning was used as a lubricant. The thermocouple (Type J) mounted on the surface of the specimen provided the temperature reading. Before performing the experiment, the specimen was heated to the desired temperature and held at that temperature for at least 30 minutes to maintain the uniformity of the temperature throughout the specimen.

2.4. Dynamic compression experiments at room temperature

Dynamic compression experiments were performed to investigate the behavior of HNBR exposed to high strain-rates. These experiments were performed using a conventional split Hopkinson pressure bar (SHPB). The typical strain-rates that can be achieved using this technique range from 200 to 10^{4} s^{-1}. The details of the apparatus and the experimental procedure can be found in Khan and Liang (1999), Khan et al. (2004) and Khan and Farrokh (2006).

2.5. Recovery, relaxation and creep experiments

It is well understood that polymers exhibit time dependent viscous behavior. Earlier investigations have demonstrated that at room temperature, the total deformation of a polymer can be divided into two major portions. A viscoelastic portion, where a part of the total deformation is recoverable during and after the unloading (also called viscoelastic strain) and a viscoplastic portion, where the deformation is permanent (also called viscoplastic strain). To measure the viscoelastic and the viscoplastic strains, uniaxial compression experiments at three different strain-rates of 10^{0}, 10^{-2} and 10^{-4} s^{-1} were performed. At each strain-rate, three different specimens were loaded to 30%, 60% and 100% true strain, respectively and then unloaded. The viscoelastic strains were obtained by recording the specimen's length as a function of time after the unloading. The measurement was continuously recorded for several weeks. The final viscoelastic strain was obtained when there was no significant change in the length of the specimen with time.

Uniaxial multi-step stress relaxation experiments at constant engineering strain-rates of 10^{0}, 10^{-2} and 10^{-4} s^{-1} were performed. At each strain-rate, the specimen was initially loaded to 25% true strain where the displacement was held constant for 30 minutes. Then the loading was continued to a true strain level of 50%, where the displacement was again held constant for another 30 minutes. This process was followed at 75% true strain, ultimately loading the sample to 100% true strain before unloading.

Uniaxial multi-step creep experiments were performed in a similar way to the relaxation experiments, except that during the creep experiments the load was held constant at true strain levels of 25%, 50% and 75% for 30 minutes each, ultimately loading the sample to 100% true strain before unloading.

2.6. Dynamic tensile experiments at room temperature

A tensile split Hopkinson pressure bar (TSHPB) is similar to the conventional spilt Hopkinson pressure bar with the differences that due to the specific design of its striker and an anvil, a tensile elastic wave is generated in the incident bar; this causes the specimen to undergo direct tensile deformation. The apparatus comprises of a gas gun, a tube striker, an anvil, a solid incident bar, a hollow (tube) transmitted bar, and a moment trap bar. In the experimental setup as shown in Fig. 1, the hollow striker tube is propelled from a gas gun, while sliding over a portion of the solid incident bar; the striker then impacts an anvil which is attached to the end of the incident bar. Due to the impact, a tensile elastic pulse (incident pulse) is generated in the incident bar while the corresponding elastic strain is measured through a high elongation uniaxial strain gage (G1) mounted on this bar. A portion of the incident pulse traveling towards the specimen gets reflected partly

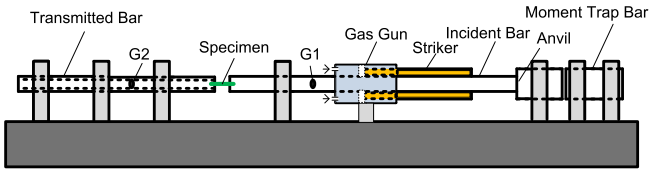

Fig. 1. Schematic of tensile split Hopkinson pressure bar (SHPB).

(compressive in nature) from the incident bar-specimen interference due to material and geometry mismatch. The remaining portion of the incident pulse (tensile in nature) gets transmitted through the specimen to the transmitted bar. The resulting strains from these reflected and transmitted pulses are measured by high elongation uniaxial strain gages, G1 and G2, respectively. In the current setup, the length and the diameter of the incident bar is 1.83 m (72 in.) and 25.4 mm (1 in.), respectively. The striker tube is 0.66 m (26 in.) long with a 38 mm (1.5 in.) outer diameter and a 6.35 mm (0.25 in.) wall thickness. All bars, the anvil and striker tube are made of Al 6061-T651.

Due to significant difference between the strength of the transmitted bar and the material being tested (e.g., low-strength, low-impedance HNBR 7530), the measured signal of the transmitted pulses were significantly weak. In order to increase the signal strength of the transmitted strain/pulse under the same stress level, either the Young's modulus of the bar material, or the cross-sectional area ratio of transmitted bar to that of the specimen, or both, need to be decreased (Chen et al., 1999). To increase the magnitude of the transmitted strain, a hollow tube with the outer diameter of 25.4 mm (1 in.) and wall thickness of 3.175 mm (0.125 in.). The length of the transmitted bar is 1.2 m (47 in.) and is made of same material as the incident bar. The specimens were dog-bone samples with the gage length of 14 mm (0.55 in.) and the cross-sectional area of 160 mm^2. The detail formulation for the direct TSHPB can be found in Chen et al. (1999).

3. Experimental results and discussion

Figs. 2–4 show the room temperature loading–unloading responses of HNBR at constant engineering strain-rates of 10^0, 10^{-2} and 10^{-4} s^{-1} respectively. The results show the repeatability between different samples of the same material. It is observed that the work hardening responses of HNBR A (hard polymer) is slightly non-linear to 45% true strain followed by the highly non-linear response to 100% true strain. However, the work hardening response

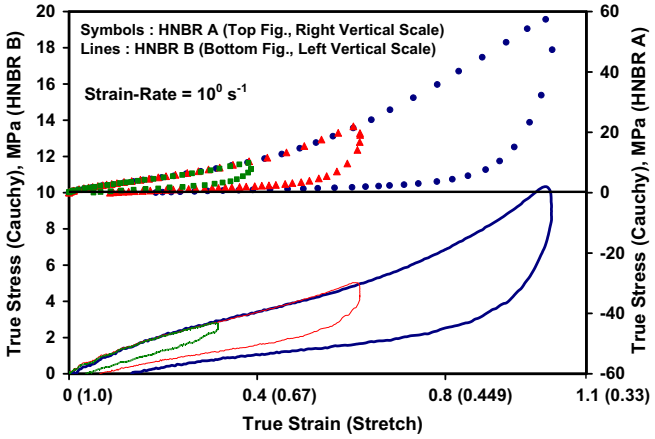

Fig. 2. True stress–strain (loading–unloading) responses of HNBR A (hard) and HNBR B (soft) polymer at a strain-rate of 10^0 s^{-1}. The numbers in the brackets corresponds to the stretch.

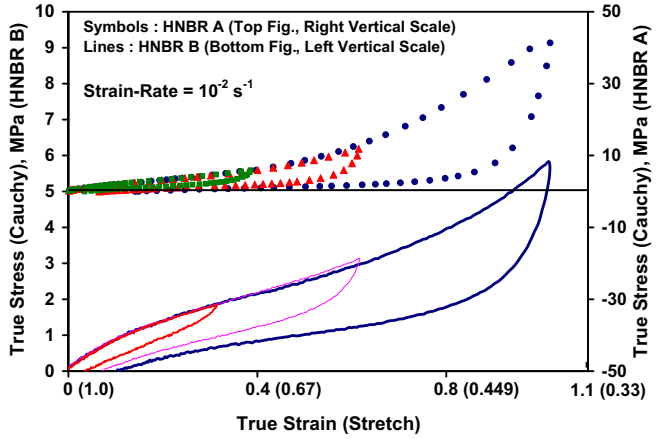

Fig. 3. True stress–strain (loading–unloading) responses of HNBR A (hard) and HNBR B (soft) polymer at a strain-rate of 10^{-2} s^{-1}.

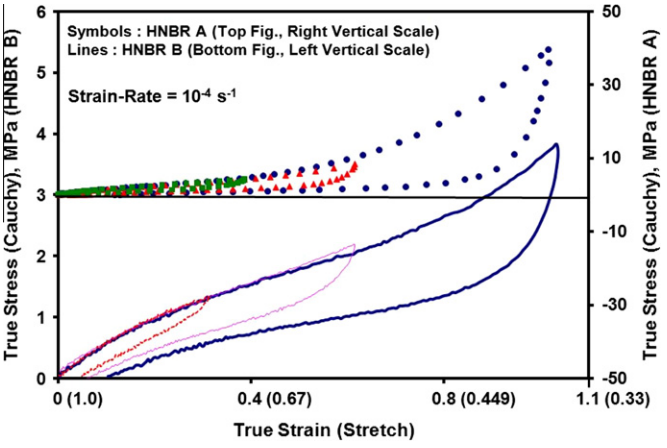

Fig. 4. True stress–strain (loading–unloading) responses of HNBR A (hard) and HNBR B (soft) polymer at a strain-rate of 10^{-4} s^{-1}.

of HNBR B (soft polymer) is observed to be non-linear throughout the deformation process. At each strain-rate, the recoverable viscoelastic strain was obtained by measuring the length of the specimen for several weeks after the experiment was performed. The final viscoelastic and viscoplastic strains were obtained from the maximum strain recovered and the amount of permanent strain present in the sample, respectively.

Fig. 5 shows the true viscoplastic strain as a function of the total true strain at different strain-rates. It is observed that out of 104% total true strain, a maximum viscoplastic strain of 0.8% and 3.16% was present in HNBR B and HNBR A, respectively. Based on this observation it is assumed that the HNBR (A and B) used in the present study exhibits almost purely viscoelastic behavior. From the figure, it is clear that the viscoplastic strain is strain-rate dependent. The viscoplastic strains observed in both the elastomers decreases with an increase in strain-rate.

Fig. 6 shows the true viscoelastic strain as a function of total true strain. From the figure, it is obvious that the fraction of true viscoelastic strain observed in both the elastomers (HNBR A and HNBR B), as a function of total strain, is independent of loading rate. Based on the results from Figs. 6 and 7, it is assumed that the material (HNBR) used in the present investigation is a purely viscoelastic material. Hence, decomposition of the total strain into viscoelastic and viscoplastic parts is ignored further in the present study.

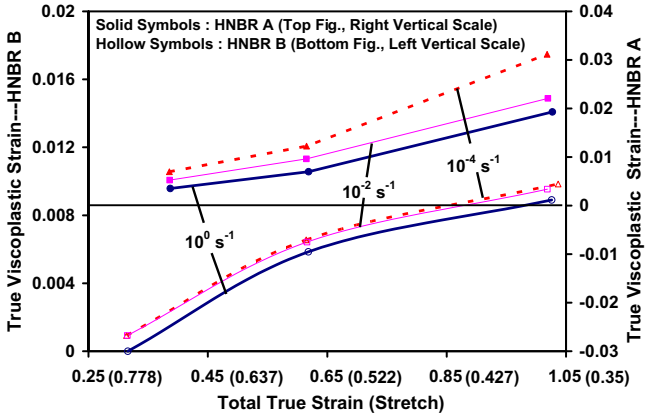

Fig. 5. Total true strain and viscoplastic strain at room temperature and at different strain-rates.

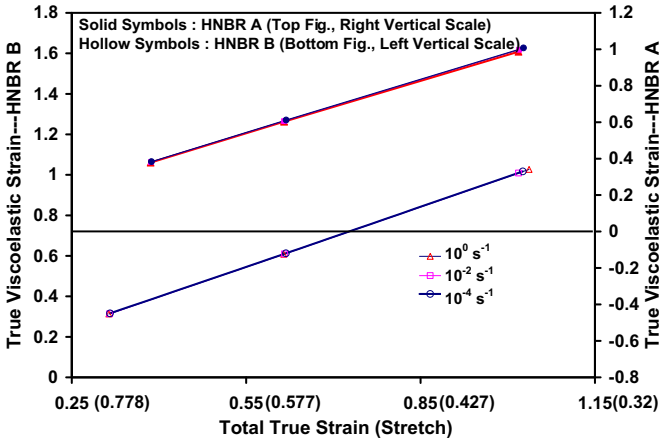

Fig. 6. Total true strain and viscoelastic strain at room temperature and at different strain-rates.

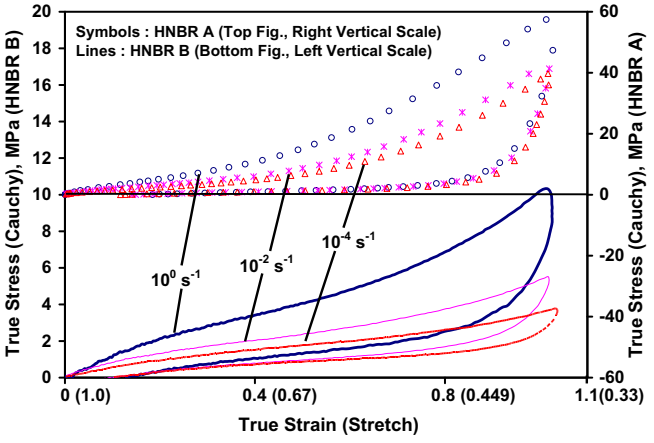

Fig. 7. True stress–strain responses of HNBR A (hard) and HNBR B (soft) polymer at room temperature and at different engineering strain-rates.

Fig. 7 shows the true stress–strain responses of HNBR at room temperature and at different strain-rates. The stress–strain curves illustrate significant work hardening behavior to 50% true strain for HNBR B and 45% true strain for HNBR A. However, the work hardening increases non-linearly in both the elastomers as the true strain exceeds this level of deformation. Also, the level of non-linearity increased with strain-rate. From the figure, it is clear that the HNBR elastomers (A and B) exhibit strong positive strain-rate sensitivity. The unloading response of HNBR A appears to be somewhat independent of strain-rate. This unloading behavior was not observed in HNBR B.

Fig. 8 illustrates the uniaxial tensile stress–strain responses of the elastomers, subjected to different strain rates. From the figure, it is demonstrated that the experiments are repeatable at the conducted strain rate. The stress–strain curves of both the elastomers, illustrate linear work hardening behavior throughout the deformation process. This result is expected because from Fig. 8, it is noticed that HNBR exhibited a small non-linear work hardening behavior in the small deformation regime.

High strain-rate compressive responses of both the elastomers are shown in Fig. 9. As reported by other researchers, it is clear that the HNBR elastomers exhibited change in the material responses from "rubbery" at quasi-static strain-rates (10^{-4} to 10^{0} s^{-1}) to "glassy" at high strain-rates (>10^{3} s^{-1}). The work hardening behavior increased with strain-rate.

High temperature (348–450 K) responses at a constant strain-rate of 10^{-2} s^{-1} are shown in Fig. 10. It is obvious that HNBR retains its elastic properties even when exposed to high temperature. This is concluded because after unloading, the amount of viscoelastic and viscoplastic strain present in the material is equal to the amount present in the sample experimented at room temperature. Also, from the figure it is observed that HNBR (A and B) does not exhibit significant temperature sensitivity up to 50% true strain. However, the temperature sensitivity was observed to increase as the deformation exceeds this level of strain. Comparing Figs. 8 and 11, it is clear that the material (HNBR) exhibits more pronounced strain-rate sensitivity effect than temperature sensitivity.

Fig. 11 shows the responses of HNBR (A and B) at 450 K and at different strain-rates. It is observed that, the material exhibits positive strain-rate sensitivity at high temperature. As shown in the figure, the rate sensitivity is more pronounced during loading than unloading for both the polymers. Also, at a strain-rate of 10^{-4} s^{-1}, HNBR B exhibited a stiffer response and the stress value at true strain of 100% exceeds the stress value at a strain-rate of 10^{-2} s^{-1} at same strain level. However, this behavior may be due to a long time exposure of the specimen (HNBR B) to a high temperature of 450 K. However, this behavior was not observed in the case of HNBR A. It should be pointed out that the specimen (HNBR B) fractured while unloading at the strain-rate of 10^{-4} s^{-1}.

Fig. 12 shows the relaxation responses at room temperature and at different strain-rates. From this figure, it is observed that the stress relaxation responses are dependent on strain-rate and the

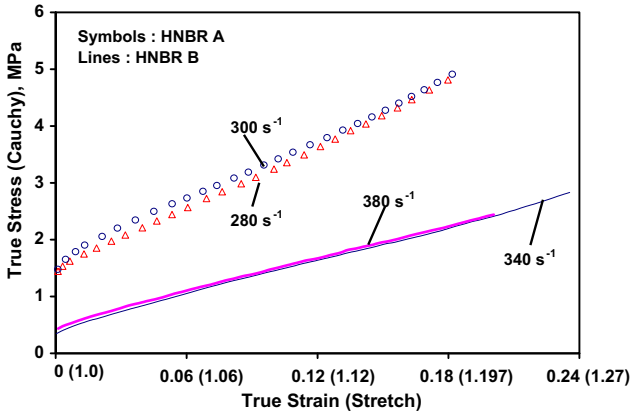

Fig. 8. True stress–strain responses of HNBR A (hard) and HNBR B (soft) polymer under dynamic tensile loading at room temperature and at different engineering strain-rates.

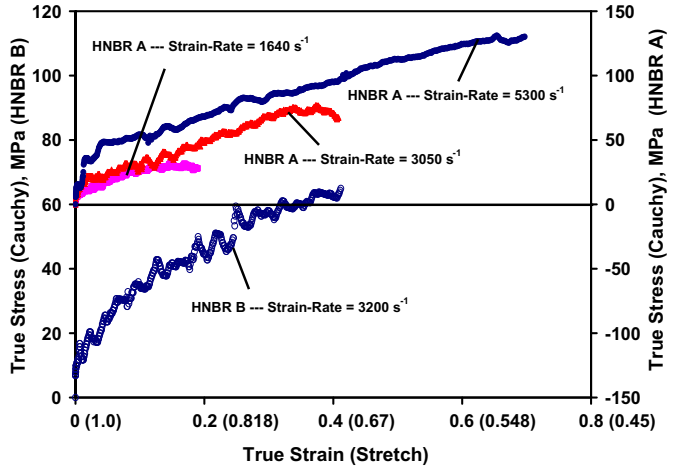

Fig. 9. True stress–strain responses of HNBR A (hard) and HNBR B (soft) polymer under dynamic compression loading at room temperature and at different engineering strain-rates.

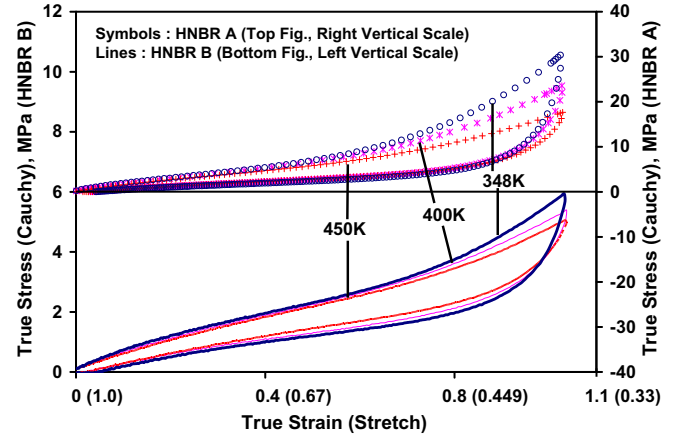

Fig. 10. True stress–strain responses of HNBR A (hard) and HNBR B (soft) polymer at different temperatures and at a constant engineering strain-rate of 10^{-2} s^{-1}.

strain-level at which the relaxation process was initiated. From a more detailed information regarding the stress drop versus the hold time as shown in Fig. 13 (for HNBR B) and Fig. 14 (for HNBR A), it is noticed that the instantaneous stress drop is dependent on strain-rate and the strain-level. The initial instantaneous relaxation response appears to be strongly dependent on strain-rate. However, after 5 minutes of relaxation, the stress drop reaches an equilibrium state and is dependent on the strain-level at which the relaxation process was initiated.

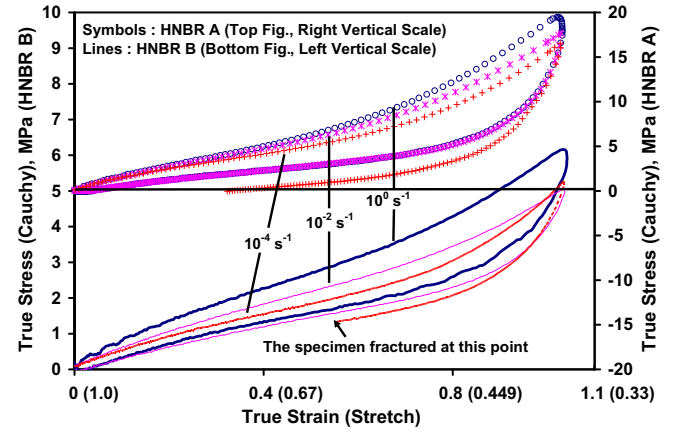

Fig. 11. True stress–strain responses of HNBR A (hard) and HNBR B (soft) polymer at 450 K and at different engineering strain-rates.

The experimental responses during creep loading at different strain-rates are shown in Fig. 15. From the figure, it is observed that the creep responses of HNBR are dependent on the strain-rate and the strain level. However, from the true strain versus time responses of HNBR B and HNBR A at different strain-rates in Figs. 16 and 17, it is clear that HNBR elastomer exhibits instantaneous creep behavior dependent on the strain-rate. Also similar to the relaxation responses, the creep responses reach an equilibrium state in 300 seconds after the process has been initiated. It is observed that, the creep responses during the equilibrium state are also dependent on strain-rate.

Fig. 18 shows the comparison of various loading conditions at a constant strain-rate of 10^0 s^{-1}. From the figure it appears that the relaxation process does not change the internal structure of HNBR B and HNBR A. This is because the relaxation responses of both the elastomers are similar to the responses during the monotonic loading. However, when comparing the creep responses with monotonic loading, the internal structure of HNBR B appears to undergo a change. This difference could also be due to insufficient loading time during the creep experiments.

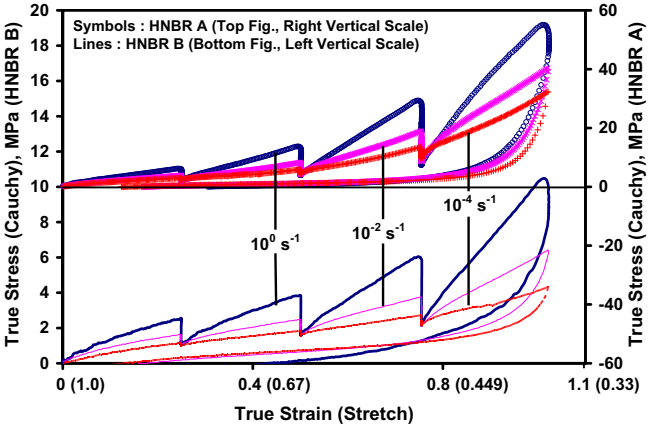

Fig. 12. True stress–strain responses of HNBR A (hard) and HNBR B (soft) polymer during the relaxation experiments at room temperature and at different engineering strain-rates.

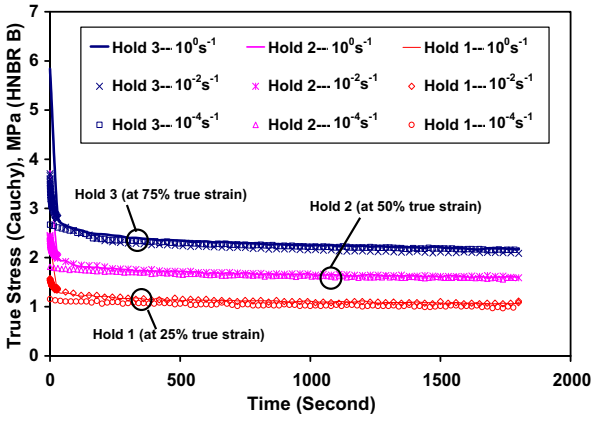

Fig. 13. True relaxation stress vs. time responses of HNBR B (soft polymer) during the relaxation experiments at room temperature and at different engineering strain-rates.

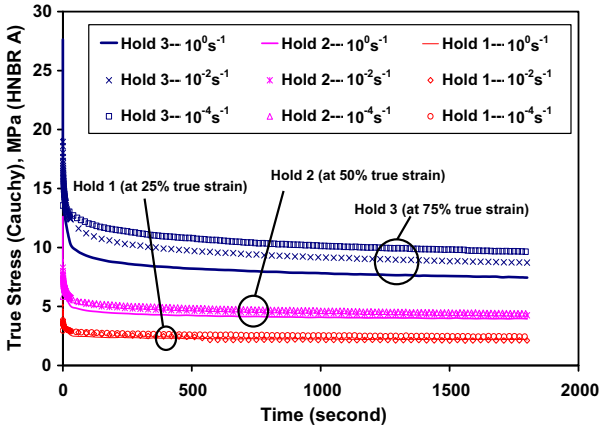

Fig. 14. True relaxation stress vs. time responses of HNBR A (hard polymer) during the relaxation experiments at room temperature and at different engineering strain-rates.

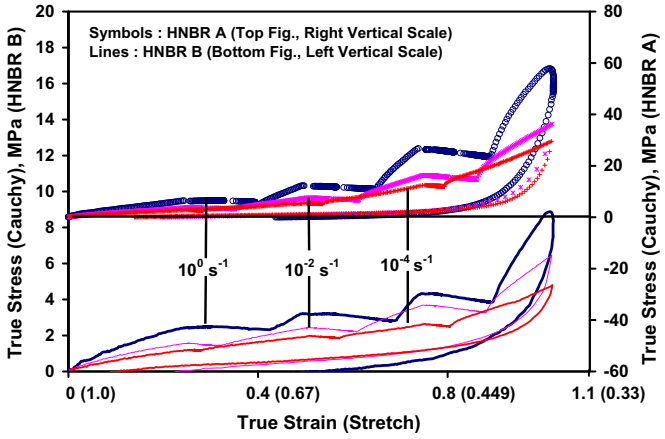

Fig. 15. True stress–strain responses of HNBR A (hard) and HNBR B (soft) polymer during the creep experiments at room temperature and at different engineering strain-rates.

Fig. 19 shows the responses of HNBR B and HNBR A subjected to various loading conditions at 450 K at a constant strain-rate of $10^{-2}\,s^{-1}$. From the figure, it is clear that, the responses of HNBR A are not influenced by loading conditions. Hence, it is demonstrated that HNBR A retains its properties when exposed to high temperatures. However, HNBR B exhibits stiffer responses under

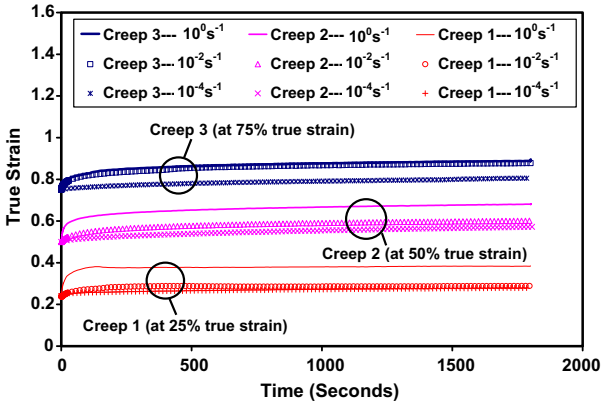

Fig. 16. True creep strain vs. time responses of HNBR B (soft polymer) during the creep experiments at room temperature and at different engineering strain-rates.

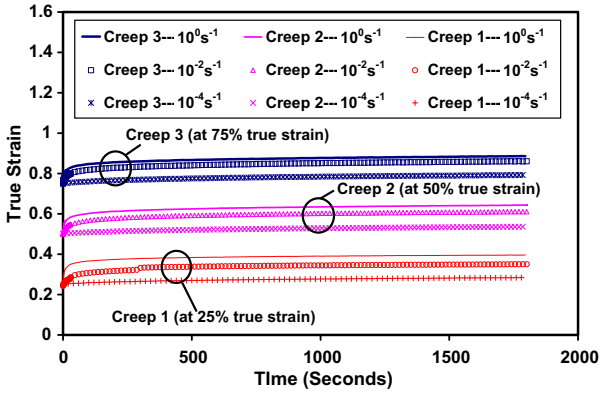

Fig. 17. True creep strain vs. time responses of HNBR A (hard polymer) during the creep experiments at room temperature and at different engineering strain-rates.

relaxation and creep loading conditions compared to monotonic loading at same strain-rate.

Figs. 20 and 21 show the relaxation and creep responses of HNBR B and HNBR A at high temperature. Since these experiments were performed at a constant engineering strain-rate, the relaxation and creep responses are found to be dependent on the level of strain at which these phenomenon were initiated. The creep

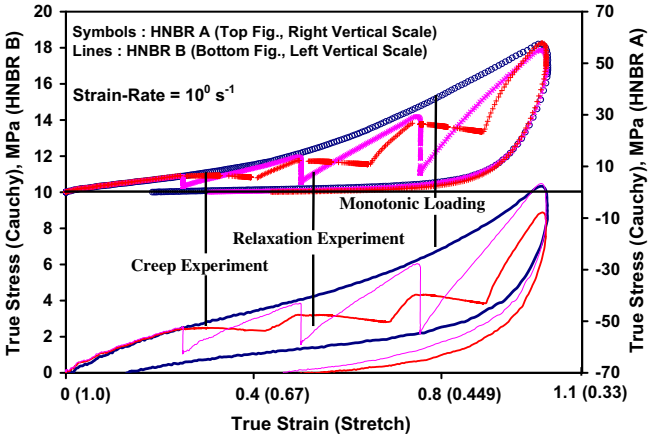

Fig. 18. A comparison of different loading condition at room temperature and at a constant engineering strain-rate of $10^{0}\,s^{-1}$.

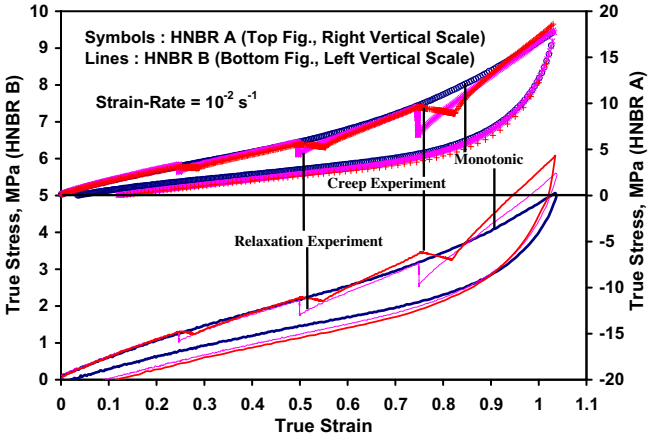

Fig. 19. A comparison of different loading condition at 450 K and at a strain-rate of $10^{-2}\,s^{-1}$.

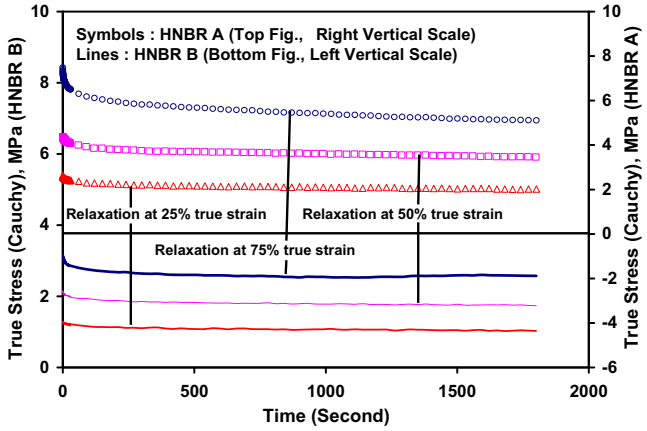

Fig. 20. True relaxation stress vs. time responses of HNBR A (hard) and HNBR B (soft) during the relaxation experiments at 450 K and at a constant engineering strain-rate of $10^{-2}\ s^{-1}$.

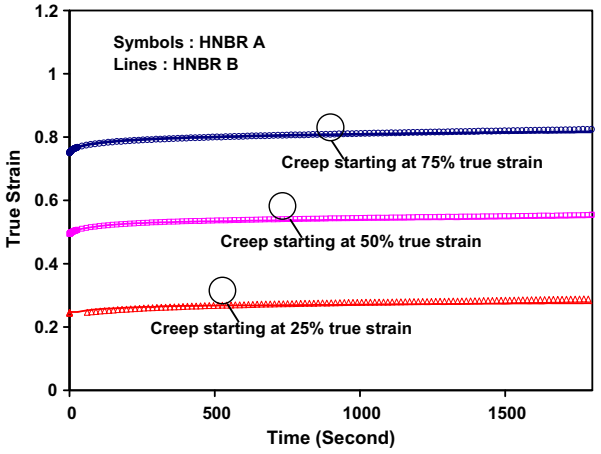

Fig. 21. True creep strain vs. time responses of HNBR A (hard) and HNBR B (soft) during the creep experiment at 450 K and at a constant strain-rate of $10^{-2}\ s^{-1}$.

and relaxation experiments, at high temperature (450 K) and at different strain-rates will be conducted in the future.

4. Conclusions

The comprehensive uniaxial responses of the elastomers, HNBR B and HNBR A over wide ranges of strain-rates and temperatures were presented. The elastomers were found to exhibit significant work hardening behavior (linear) to 50% true strain and the work hardening rate increased non-linearly after this deformation. Strain-rate sensitivity was found to be more pronounced than temperature sensitivity. The elastomer exhibits change in its behavior from rubbery at low strain-rates to glassy at high rates of deformation. The instantaneous stress drop during the stress relaxation experiment was found to be strain-rate dependent and the stress drop during the equilibrium state was found to be dependent on the strain level at which the relaxation phenomenon started.

Acknowledgement

The first and last authors appreciate the financial support of Halliburton Energy Services for this project.

References

Ames, N.M., Srivastava, V., Chester, S.A., Anand, L., 2009. A thermo-mechanically coupled theory for large deformations of amorphous polymers. Part II: applications. International Journal of Plasticity 25, 1495–1539.
Anand, L., Ames, N.M., Srivastava, V., Chester, S.A., 2009. A thermo-mechanically coupled theory for large deformations of amorphous polymers. Part I: formulation. International Journal of Plasticity 25, 1474–1494.
Bardenhagen, S.G., Stout, M.G., Gray, G.T., 1997. Three-dimensional, finite deformation, viscoplastic constitutive models for polymeric materials. Mechanics of Materials 25, 235–253.
Beda, T., 2007. Modeling hyperelastic behavior of rubber: a novel invariant-based and a review of constitutive models. Journal of Polymer Science: Part B: Polymer Physics 45, 1713–1732.
Bergström, J.S., Boyce, M.C., 1998. Constitutive modeling of the large strain time-dependent behavior of elastomers. Journal of Mechanics and Physics of Solids 46 (5), 931–954.
Bird, R.B., Armstrong, R.C., Hassager, O., 1977. Dynamics of Polymeric Liquids, vol. 1. John Wiley and Sons, New York.
Chen, W., Zhang, B., Forrestal, M.J., 1999. A split Hopkinson bar technique for low-impedance materials. Experimental Mechanics 39 (2), 81–85.
Fatt, M.S.H., Ouyang, Xin., 2008. Three-dimensional constitutive equations for styrene butadiene rubber at high strain rates. Mechanics of Materials 40, 1–16.
Haupt, P., Lion, A., Backhaus, E., 2000. On the dynamic behavior of polymers under finite strains: constitutive modeling and identification of parameters. International Journal of Solids and Structures 37, 3633–3646.
Jerrams, S.J., Kaya, M., Soon, K.F., 1998. The effects of strain rate and hardness on the material constants of nitrile rubbers. Materials and Design 19, 157–167.
Khan, A.S., Farrokh, B., 2006. Thermo-mechanical response of nylon 101 under uniaxial and multi-axial loadings: Part I. Experimental results over wide ranges of temperatures and strain rates. International Journal of Plasticity 22, 1506–1529.
Khan, A.S., Liang, R., 1999. Behavior of three BCC metal over a wide range of strain rates and temperatures. International Journal of Plasticity 15, 1089–1109.
Khan, A.S., Pamies, O.L., 2002. Time and temperature dependent response and relaxation of a soft polymer. International Journal of Plasticity 18, 1359–1372.
Khan, A.S., Zhang, H., 2001. Finite deformation of polymer and constitutive modeling. International Journal of Plasticity 17, 1167–1188.
Khan, A.S., Pamies, O.L., Kazmi, R., 2006. Thermo-mechanical large deformation response and constitutive modeling of viscoelastic polymers over a wide range of strain rates and temperatures. International Journal of Plasticity 22, 581–601.
Khan, A.S., Suh, Y.S., Kazmi, R., 2004. Quasi-static and dynamic loading responses and constitutive modeling of titanium alloys. International Journal of Plasticity 20, 2233–2248.
Qi, H.J., Boyce, M.C., 2005. Stress–strain behavior of thermoplastic polyurethanes. Mechanics of Materials 37, 817–839.
Regrain, C., Laiarinandrasana, L., Toillon, S., Saï, K., 2009. Multi-mechanism models for semi-crystalline polymer: constitutive relations and finite element implementation. International Journal of Plasticity 25, 1253–1279.
Spathis, G., 1995. Non-Gaussian stress–strain constitutive equation for crosslinked elastomers. Polymer 36 (2), 309–313.
Spathis, G., Kontou, E., 2008. Modeling of nonlinear viscoelasticity at large deformations. Journal of Material Sciences 43, 2046–2052.
Zaïri, F., Naït-Abdelaziz, M., Gloaguen, J.M., Lefebvre, J.M., 2008. Modelling of the elasto-viscoplastic damage behaviour of glassy polymer. International Journal of Plasticity 24, 945–965.